

Green and sustainable method of manufacturing anti-fouling zwitterionic polymers-modified poly(vinyl chloride) ultrafiltration membranes

*Original*

Green and sustainable method of manufacturing anti-fouling zwitterionic polymers-modified poly(vinyl chloride) ultrafiltration membranes / Xie, W.; Tiraferri, A.; Ji, X.; Chen, C.; Bai, Y.; Crittenden, J. C.; Liu, B.. - In: JOURNAL OF COLLOID AND INTERFACE SCIENCE. - ISSN 0021-9797. - 591:(2021), pp. 343-351. [10.1016/j.jcis.2021.01.107]

*Availability:*

This version is available at: 11583/2872988 since: 2021-03-03T10:15:43Z

*Publisher:*

Academic Press Inc.

*Published*

DOI:10.1016/j.jcis.2021.01.107

*Terms of use:*

This article is made available under terms and conditions as specified in the corresponding bibliographic description in the repository

*Publisher copyright*

Elsevier postprint/Author's Accepted Manuscript

© 2021. This manuscript version is made available under the CC-BY-NC-ND 4.0 license  
<http://creativecommons.org/licenses/by-nc-nd/4.0/>. The final authenticated version is available online at:  
<http://dx.doi.org/10.1016/j.jcis.2021.01.107>

(Article begins on next page)

1 Green and sustainable method of manufacturing  
2 anti-fouling zwitterionic polymers-modified  
3 poly(vinyl chloride) ultrafiltration membranes

4 *Wancen Xie<sup>a,b</sup>, Alberto Tiraferri<sup>c</sup>, Xuanyu Ji<sup>a,b</sup>, Chen Chen<sup>d</sup>, Yuhua Bai<sup>e</sup>, John C. Crittenden<sup>f</sup>,*  
5 *and Baicang Liu<sup>\*,a,b</sup>*

6 <sup>a</sup> Key Laboratory of Deep Earth Science and Engineering (Ministry of Education), College of  
7 Architecture and Environment, Institute of New Energy and Low-Carbon Technology, Sichuan  
8 University, Chengdu 610207, PR China

9 <sup>b</sup> Yibin Institute of Industrial Technology, Sichuan University Yibin Park, Yibin, 644000, PR  
10 China

11 <sup>c</sup> Department of Environment, Land and Infrastructure Engineering, Politecnico di Torino, Corso  
12 Duca degli Abruzzi 24, 10129 Turin, Italy

13 <sup>d</sup> Litree Purifying Technology Co., Ltd, Haikou, Hainan 571126, PR China

14 <sup>e</sup> Infrastructure Construction Department, Chengdu University, Chengdu 610106 PR China

---

\* Corresponding author.

E-mail: [bcliu@scu.edu.cn](mailto:bcliu@scu.edu.cn); Tel: +86-28-85995998; Fax: +86-28-62138325.

15 <sup>f</sup> Brook Byers Institute for Sustainable Systems, School of Civil and Environmental Engineering,  
16 Georgia Institute of Technology, Atlanta, GA 30332, USA

17

18

19

20

21

22

23

24

25

26

27

28

29

30

31

32

33

34

35

36

37

## 38 **Abstract**

39 The nonsolvent induced phase separation (NIPS) method for ultrafiltration (UF) membrane  
40 fabrication relies on the extensive use of traditional solvents and toxic chemicals, thus ranking  
41 first in terms of ecological impacts among all the membrane fabrication steps. Methyl-5-  
42 (dimethylamino)-2-methyl-5-oxopentanoate (PolarClean), as a green solvent, was utilized in this  
43 study to fabricate poly(vinyl chloride) (PVC) UF membranes. Subsequently, in post-treatment  
44 process, a zwitterionic polymer, [2-(methacryloyloxy) ethyl] dimethyl-(3-sulfopropyl)  
45 ammonium hydroxide (DMAPS), was grafted onto the membrane surface to enhance its anti-  
46 fouling properties. This step was achieved using a surface-initiated activator regenerated by  
47 electron transfer-atom transfer radical polymerization (ARGET-ATRP) reaction, with a greener  
48 activator compared to traditional ones. This novel method used low toxicity chemicals, thus  
49 avoiding the environmental hazards of traditional ATRP and greatly improving the reaction  
50 efficiency. We systematically studied the grafting time effect on the resulted membranes using  
51 sodium alginate as the foulant, and found that short grafting time (30 minutes) achieved excellent  
52 membrane performance: pure water permeability of  $2872 \text{ L m}^{-2} \text{ h}^{-1} \text{ bar}^{-1}$ , flux recovery ratio of  
53 86.4 % after 7-hour fouling test, and foulant rejection of 96.0 %. This work discusses for the first  
54 time an approach with low environmental impacts to both fabricate and modify PVC UF  
55 membranes.

## 56 **Keywords**

57 Poly(vinyl chloride) PVC; Ultrafiltration; Green solvent; ARGET-ATRP; DMAPS

## 58      **1. Introduction**

59            Poly(vinyl chloride) (PVC), the second largest manufactured resin by volume worldwide [1,  
60 2], is also one of the most common polymers applied to fabricate ultrafiltration (UF) membranes  
61 due to numerous characteristics (*e.g.*, low-cost, suitable mechanical strength, and acid-alkali-  
62 microbial resistance [3-6]). Unfortunately, the intrinsic hydrophobic properties of PVC increase  
63 the likelihood of membrane contamination [4, 7], leading to low flux and reduced life-time. This  
64 mechanism limits PVC application in the membrane field. To improve the antifouling property  
65 of PVC membranes, hydrophilic enhancement is essential [8].

66            Blending [9-11], surface grafting [12-14], and surface coating [15] are typical modification  
67 strategies to improve the hydrophilicity of membranes. Blending entails adding hydrophilic  
68 materials during the membrane casting process. Blending is a convenient method, but not  
69 without important restrictions: adequate solubility of the additives in the solvent is required [16],  
70 and complete coverage of the membrane surface with the additives is usually difficult to achieve  
71 [17, 18]. As for surface grafting, this procedure allows the formation of consistent hydrophilic  
72 layers on membrane surfaces, as well as the preservation of membrane physical properties [17].  
73 A considerable number of hydrophilic polymers have been studied for grafting purposes and the  
74 feasibility of this method has been widely discussed. The literature contains reports on  
75 poly(vinylidene fluoride) (PVDF) [19, 20], polyethersulfone (PESU) [21], polysulfone (PSU)  
76 [22], and cellulose-based membranes [12, 23] modified via surface grafting by atom transfer  
77 radical polymerization (ATRP) reaction. For PVDF membranes, the typical steps include  
78 grafting hydrophilic polymers on membrane surfaces pre-coated with biophenols (*e.g.*,  
79 polydopamine, tannic acid), which provide active sites for the reaction [17, 19]. However, this  
80 approach reduces the permeability of UF membranes due the pore occlusion [24, 25]. Therefore,

81 direct grafting of hydrophilic materials to the membrane surface may be a better option for which  
82 it is possible to exploit the halogen atoms present in the membrane backbones (*e.g.*, PVDF and  
83 PVC membranes).

84 To the best of our knowledge, only a few works have attempted direct grafting of hydrophilic  
85 materials to the PVC membrane surfaces [16, 26-29]. Cheng *et al.* [16] grafted poly(2-  
86 hydroxyethylmethacrylate) (PHEMA) and poly(1-butyl-3-vinylimidazolium bromide) (PBVIm-  
87 Br) on PVC membrane via a 2-step ATRP reaction. This modification method was time-  
88 consuming, because for each ATRP step takes at least six hours. moreover, various different  
89 chemicals were used in the polymerization process, involving toxic ones. However, the resulting  
90 membrane showed low pure water flux ( $\sim 100 \text{ L/m}^2\cdot\text{h}$ ) and unsatisfactory anti-fouling properties  
91 (flux recovery ratio of 79.7% after only 100-min fouling test). Other works included hydrophilic  
92 materials such as N-vinyl-2-pyrrolidinone (NVP) [26], ethylenediamine (EDA),  
93 diethylenetriamine (DETA), pentaethylenehexamine (PEHA) [28], and poly(3-sulfopropyl  
94 methacrylate–methacryloxyethyl trimethyl ammoniumchloride–glycidyl methacrylate) (PSTG)  
95 [29]. There is no doubt that more work should be done to investigate more efficient materials for  
96 the surface grafting of PVC membranes via greener modification strategies.

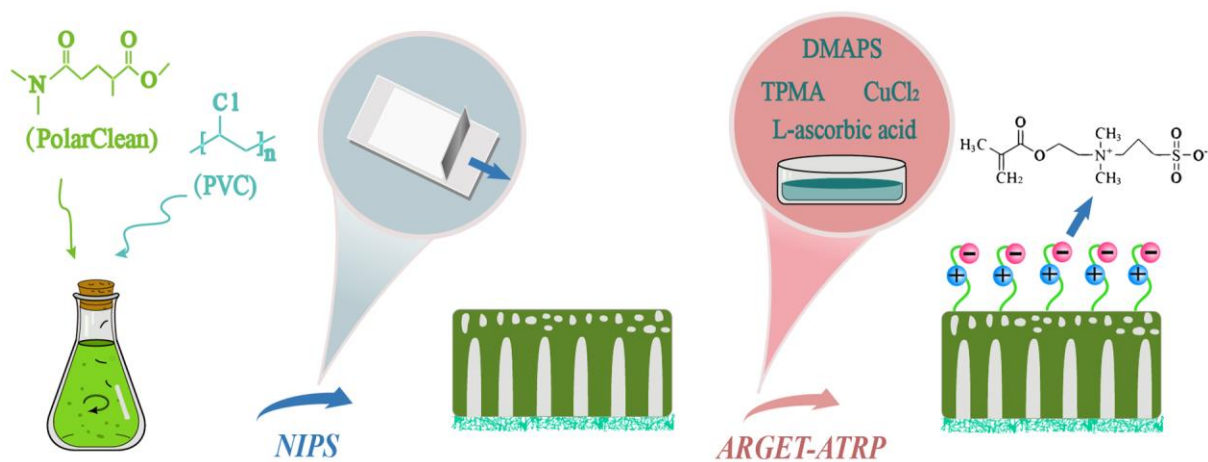
97 Zwitterionic polymers have attracted great attention in recent years as modification  
98 materials, owing to their hydrophilicity, blood compatibility, and environmental stability [23, 30,  
99 31]. These polymers are composed by the same number of cationic and anionic groups, thus  
100 displaying overall neutral potential, and promote a hydration layer around the brushes to  
101 significantly reduce membrane fouling [17, 31]. Among zwitterionic polymers, [2-  
102 (methacryloyloxy) ethyl] dimethyl-(3-sulfopropyl) ammonium hydroxide (DMAPS) was studied  
103 by Zhou *et al.* [32] and was found to be the best performing one in terms of antifouling ability

104 among 66 monomers used to modify PESU membranes. In addition, DMAPS does not pose  
105 dangersto human health and to the environment according to Safety Data Sheet, thus conforming  
106 to the principles of green chemistry [33]. There have been works on poly(vinylidene fluoride)  
107 (PVDF) [17, 19, 34], polysulfone (PSU) [22], PESU [21], aliphatic polyketone (PK) [35],  
108 regenerated cellulose (RC) [36], and poly(lactic acid) (PLA) membranes [37], as well as  
109 aromatic polyamide reverse osmosis (RO) membranes [38] and thin-film composite (TFC)  
110 forward osmosis (FO) membranes [39] modified by grafting DMAPS, all of which demonstrated  
111 improved antifouling properties. However, no PVC membrane has been modified with this  
112 molecule, implying a significant deficiency in the field.

113 The activator regenerated by electron transfer-atom transfer radical polymerization  
114 (ARGET-ATRP) reaction is the recent development of ATRP [40], and it can be used to graft  
115 polymer brushes to the membrane surface. Our previous studies [9, 41, 42] utilized traditional  
116 ATRP to obtain copolymer PVC-g-graft-poly(ethylene glycol) methyl ether methacrylate (PVC-  
117 g-PEGMA), which needed alkyl halide (-Cl) ligand and a relatively high concentration of a  
118 transition metal catalyst at lower oxidation state ( $\text{Cu}^{\text{I}}$ ) to initiate the reaction. In such reaction  
119 process, the oxygen must be carefully removed, and high temperature and long polymerization  
120 times are required. To avoid these limitations, ARGET-ATRP may be adopted, in which the  
121 catalyst is continuously regenerated by a reducing agent from  $\text{Cu}^{\text{II}}$  species [40, 43, 44].  
122 Therefore, only ppm levels of the catalysts are required, and a limited amount of air can be  
123 present. Meanwhile, more active ligands can improve the efficiency of the polymerization  
124 system, allowing the reaction at room temperature with shortened reaction time [45, 46].  
125 Therefore, ARGET-ATRP is considered a grafting method with lower environmental impacts.  
126 [40, 43, 44].

127 When PVC membranes are prepared via NIPS process, large amounts of organic solvents (*e.g.*,  
128 1-methyl-2-pyrrolidinone) are needed, which are toxic to human and the environment [47-49],  
129 thus violating the principles of green chemistry [50-53]. Therefore, green and sustainable  
130 solvents are urgently needed to replace traditional ones [54]. Our previous study [55] used  
131 PolarClean for PVC membrane fabrication. This compound has no health hazards, and much  
132 lower environmental impacts compared to other common membrane preparation solvents [56-61].  
133 Additionally, it is nonflammable and improves the safety of the whole membrane fabrication  
134 process [62, 63]. The PVC membrane prepared by PolarClean in the previous study had ultrahigh  
135 pure water permeability and sodium alginate (SA) rejection, but the antifouling property was  
136 relatively poor (flux recovery ratio of 57 % after a 7-hour fouling test) [55]. Therefore, in the  
137 present work, PolarClean was also utilized to prepare PVC membranes, but we significantly  
138 improved the environmental compatibility of the fabrication process as well as improved the  
139 antifouling properties of the membranes by grafting DMAPS monomers using sustainable  
140 ARGET-ATRP method (Fig. 1). The reaction conditions are investigated and optimized to obtain  
141 widely applicable PVC membranes with all-round high performance.

142





143 **Fig. 1.** Schematic overview of the membrane fabrication strategy: dissolution of PVC in green  
144 solvent PolarClean, followed by fabrication the virgin membrane via NIPS method. Finally,  
145 DMAPS polymers were grafted on the membrane surface via ARGET ATRP method.

146

## 147 **2. Materials and methods**

### 148 **2.1. Chemicals**

149 Poly(vinyl chloride) (PVC, high molecular weight), [2-(Methacryloyloxy)ethyl]dimethyl-(3-  
150 sulfopropyl)ammonium hydroxide (DMAPS, 95%,  $M_n = 279.35$  g/mol), tris(2-  
151 pyridylmethyl)amine (TPMA, 98%), copper (II) chloride ( $\text{CuCl}_2$ ,  $\geq 99.999\%$ ), L-ascorbic acid ( $>$   
152 99%), methanol (99.9 %), sodium chloride (NaCl, reagent grade, 99%), and sodium alginate  
153 (SA, Lot# MKBL7997V) were obtained from MilliporeSigma (St. Louis, MO, USA). Ethanol  
154 (99.7%) was obtained from Chengdu Chron Chemicals Co., Ltd. (Chengdu, China). PolarClean ( $>$   
155 99.9%) was obtained from Solvay Specialty Polymers (Shanghai, China).

### 156 **2.2. Preparation of PVC membranes based on PolarClean**

157 The membrane casting solution consisted of a solution of polymer PVC (8 g) and solvent  
158 PolarClean (92 g). The membranes were fabricated via NIPS method. Poly(ethylene  
159 terephthalate) (PET) non-woven fabric was used as the backing layer. Detailed steps are  
160 presented in Text S1 (Supporting Information, SI). The PVC membranes were washed with  
161 ethanol to remove the residual solvent, and washed with deionized (DI) water to eliminate  
162 ethanol, and stored in DI water at 4 °C.

### 163 **2.3. Surface grafting of zwitterionic polymers**

164 Because of the light sensitivity property of L-ascorbic acid, TPMA and  $\text{CuCl}_2$ , the reaction  
165 was proceeded in a dark environment. 15.64 g of DMAPS monomer was dissolved in 200 mL of  
166 methanol-DI water solution (1:1 v/v) in a 1000 mL sealed glass bottle. After a 10-min nitrogen  
167 gas bubbling, 0.004 g of  $\text{CuCl}_2$  and 0.056 g of TPMA dissolved in a 8 mL of methanol-DI water  
168 mixture (1:1 v/v) were added to the solution. Another 10 min  $\text{N}_2$  bubbling was applied. The PVC  
169 membrane previously secured to a glass sheet with waterproof tape was then placed in the glass  
170 bottle, with additional 10 min  $\text{N}_2$  bubbling to remove the oxygen in this system. Subsequently,  
171 1.2 g of L-ascorbic acid in 12 mL of methanol-DI water mixture (1:1 v/v) was poured to initiate  
172 the reaction. Meanwhile,  $\text{N}_2$  was continuously bubbled to stir the solution and remove oxygen.  
173 After a designated time (30, 60, or 90 min), the bottle was open to air, and the reaction  
174 terminated. Finally, the modified membrane was thoroughly rinsed and stored in DI water at 4  
175 °C. The labels for pristine membrane and membranes fabricated with 30, 60, 90 min grafting  
176 times are M1-0 min, M2-30 min, M3-60 min, and M4-90 min, respectively.

#### 177 **2.4. Ternary phase diagram determination**

178 The cloud points for the PVC-PolarClean system were measured by titration. Different  
179 amounts of PVC (6 wt.%, 8 wt.% and 10 wt.%) were completely dissolved in PolarClean, and DI  
180 water was slowly added to the solutions at 60 °C, stirring at 500 rpm, until the solution was no  
181 longer homogeneous. As a comparison, the cloud points of PVC-DMAc and PVC-NMP systems  
182 were also measured. The results are presented in Figure S1 (SI).

#### 183 **2.5. Membrane surface characterizations**

184 The membrane morphologies were obtained by scanning electron microscopy (SEM)  
185 (REGULUS 8230, Hitachi, Japan). The surface roughness was detected by atomic force  
186 microscopy (AFM, Dimension Icon, Bruker, Germany), performed in ScanAsyst mode. The

187 chemical composition for all membranes was gotten by X-ray photoelectron spectroscopy (XPS)  
188 (Axis Supra, Kratos Analytical Ltd., UK) and fourier transform infrared (FTIR) spectrometer  
189 (Nicolet is 20, Thermo Fisher Scientific Inc., US) with an attenuated total reflection (ATR)  
190 equipment [64]. The dynamic water contact angles were measured via a KRÜSS DSA 25S  
191 measurement (KRÜSS GmbH, Germany) at room temperature. For more details, the reader can  
192 refer to our previous study [55] and Text S2 (SI).

## 193 **2.6. Ultrafiltration and anti-fouling performance assessment**

194 The membrane filtration tests were conducted using a dead-end filtration cell (Amicon 8200,  
195 Millipore, USA), which had an effective membrane area of 28.7 cm<sup>2</sup>. The pressure was set at 10  
196 psi (0.07 MPa) to conduct the tests. The permeate was weighed and recorded using a balance  
197 (Pro Balance AV8101, Ohaus Adventurer, USA) and Collect 6.1 software every minute. The  
198 temperature was 25 °C for all the tests. The detailed steps can be found in our previous study [65,  
199 66], and are in Text S3 (SI).

200 The Shimadzu total organic carbon (TOC) analyzer (Shimadzu Co., Japan) was used to  
201 measure the SA concentrations [41]. Meanwhile, the antifouling property of the membrane was  
202 characterized by the following indexes: the flux recovery ratio (FRR), the total flux decline ratio  
203 (DR<sub>t</sub>), the reversible flux decline ratio (DR<sub>r</sub>), and the irreversible flux decline ratio (DR<sub>ir</sub>) [67].

$$204 \quad \text{FRR} = \frac{J_2}{J_1} \times 100\% \quad (1)$$

$$205 \quad \text{DR}_t = \left( 1 - \frac{J_p}{J_1} \right) \times 100\% \quad (2)$$

$$206 \quad \text{DR}_r = \frac{J_2 - J_p}{J_1} \times 100\% \quad (3)$$

$$DR_{ir} = \left( 1 - \frac{J_2}{J_1} \right) \times 100\% \quad (4)$$

$J_1$ ,  $J_2$ ,  $J_p$  ( $L m^{-2} h^{-1}$ ) are the pure water flux of new membrane, the pure water flux of the membrane after physical cleaning, and the SA solution flux, respectively.

## 2.7. XDLVO theory to assess the membrane fouling potential

The membrane anti-fouling properties can also be assessed by estimation of the interfacial free energy by the extended Derjaguin, Landau, Verwey and Overbeek (XDLVO) theory, which has been widely used for the foulant-membrane interaction energy calculation, related to the fouling potential of membranes. The total interaction free energy between foulants (denoted with subscript 1) and membrane surface (subscript 2) in a medium (DI water, subscript 3) is obtained by the combination of Lifshitz–van der Waals (LW) and Lewis acid–base (AB) interaction energies [68]:

$$\Delta G_{132} = \Delta G_{132}^{LW} + \Delta G_{132}^{AB} \quad (5)$$

$$\Delta G_{132}^{LW} = -2(\sqrt{\gamma_2^{LW}} - \sqrt{\gamma_3^{LW}})(\sqrt{\gamma_1^{LW}} - \sqrt{\gamma_3^{LW}}) \quad (6)$$

$$\Delta G_{132}^{AB} = 2 \left[ (\sqrt{\gamma_3^+}(\sqrt{\gamma_1^-} + \sqrt{\gamma_2^-} - \sqrt{\gamma_3^-}) + \sqrt{\gamma_3^-}(\sqrt{\gamma_1^+} + \sqrt{\gamma_2^+} - \sqrt{\gamma_3^+}) - (\sqrt{\gamma_1^+ \gamma_2^-} + \sqrt{\gamma_1^- \gamma_2^+}) \right] \quad (7)$$

where  $\gamma^{LW}$ ,  $\gamma^+$  and  $\gamma^-$  are the Lifshitz van der Waals, electron acceptor, and electron donor components of membrane surface tension parameters, respectively. These parameter were obtained by contact angle measurements of membranes and foulants, using three probe liquids of known surface tension parameters (water, diiodomethane, and formamide in Table S1) [69, 70]; the calculation details are listed in Table S2 and Text S4 (SI). The electrostatic force (EL)

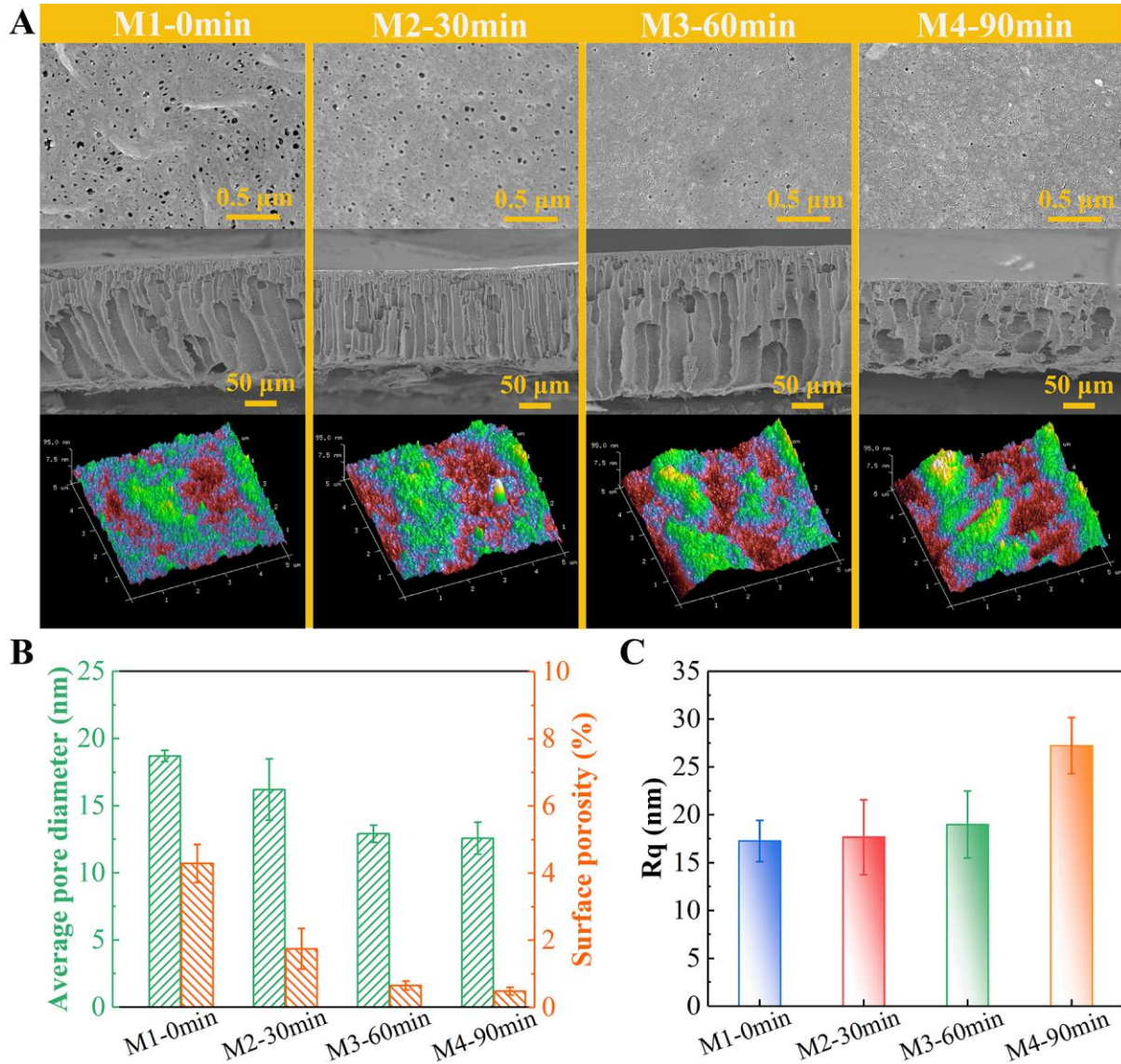
226 interaction energy ( $\Delta G_{132}^{EL}$ ) is also one component of the total interaction free energy, but it is  
227 much smaller than  $\Delta G_{132}^{LW}$  and  $\Delta G_{132}^{AB}$ , and can thus be neglected.

### 228 **3. Results and discussion**

#### 229 **3.1. Membrane morphology**

230 The surface and cross-sectional morphologies for M1-0 min, M2-30 min, M3-60 min, and M4-  
231 90 min are reported in Fig. 2A. Based on surface SEM images, it is obvious that the pore  
232 diameter and pore density were reduced with the increase of the grafting time. We used Image  
233 Pro Plus V.7.0 software (Media Cybernetics, USA) to quantify the pore diameter information  
234 and surface porosities (Fig. 2B), as well as maximum pore diameters and pore densities reported  
235 in Table S3 (SI). At least two different areas of the same membrane were included for the  
236 statistics. The average pore diameters decreased from 18.7 nm for M1-0 min to 12.6 nm for M4-  
237 90 min, along with significant reduction of surface porosities from 4.29 % for M1 to 0.49 % for  
238 M4. The gradual decrease of pore diameter and surface porosity was attributed to higher  
239 DMAPS brush thickness and grafting density resulting from longer ARGET ATRP reaction time.  
240 This phenomenon is consistent with previous reports [17, 22, 71]. This phenomenon will reduce  
241 the permeabilities of the membranes to some extent, which is discussed below. However, by  
242 prolonging the grafting time from 120 min to 180 min, the pore size and porosity did  
243 significantly decrease (Fig. S2, SI), which is probably due to the saturation of active sites. The  
244 cross-sectional SEM images revealed that this modification method had little effect on cross-  
245 sectional pore structure. The 3D AFM images and root-mean-square ( $R_q$ ) roughness values are  
246 shown in Fig. 2A,C. Overall, zwitterionic polymer brushes increased the surface roughness due  
247 to relatively uneven DMAPS layers covering the membrane surface [19]. Moreover, some

248 outshoots, which were formed by the aggregation of the grafted polymer chains, appeared on the  
 249 surfaces, thus further increasing the surface roughness [22].



250

251 **Fig. 2.** Membrane morphology. (A) Surface and cross-sectional SEM images, as well as 3D  
 252 AFM images, of PVC membranes obtained with different grafting times: M1-0 min, M2-30 min,  
 253 M3-60 min, and M4-90 min. All surface SEM images were under 50K $\times$  magnification, and the  
 254 cross-sectional images under 300 $\times$  magnification. (B) Average pore diameters and surface  
 255 porosities of M1-M4. At least two surface SEM images were analyzed for each membrane

256 sample to obtain these values. (C)  $R_q$  surface roughness values of M1-M4 calculated from AFM  
257 images. For each membrane sample, at least four different locations on the surface were probed.

### 258 3.2. Membrane surface chemistry

259 The XPS spectra of all membranes are presented in Fig. S3 (SI). For pure PVC membrane,  
260 carbon (C) and chlorine (Cl) were the dominant elements on the surface. The low content of  
261 oxygen (O) (0.5 At. %) found on the membranes is attributed to the adsorption of H<sub>2</sub>O or  
262 negligible residues of PolarClean [72]. However, after DMAPS was grafted to membrane  
263 surface, new peaks of O, nitrogen (N) and sulfur (S) were detected. We used CasaXPS  
264 processing software (Casa Software Ltd., U.K.) to estimate element atom percentages for M1-  
265 M4, with the results summarized in Table 1. Moreover, this software was also employed to carry  
266 out C 1s peak curve-fitting, and the results are shown in Fig. 3A-D. Specifically, for M1-0 min,  
267 only C-C/C-H (284.6 eV) and CHCl (285.7 eV) peaks were observed. However, after surface  
268 grafting, peaks attributed to C-N/C-O/C-S (286.4 eV) and O-C=O (288.2 eV) appeared, proving  
269 the successful grafting of DMAPS to the surfaces. As DMAPS polymers were the only source of  
270 O-C=O, the mole fraction of DMAPS can be estimated using eq. (8) [14, 66]:

$$271 \quad X^{\text{DMAPS}} = \frac{A_{\text{COO}}}{A_{\text{COO}} + A_{\text{CHCl}}} \quad (8)$$

272  $A_{\text{CHCl}}$  and  $A_{\text{COO}}$  represent the areas of CHCl and COO peaks, and corresponding results are also  
273 reported in Table 1. Compared to our previous study, which entailed the modification of PVC  
274 membranes by blending hydrophilic polymers with PVC in the casting solution [55], this grafting  
275 method was much more efficient to introduce more zwitterionic polymers on the surface, which  
276 is an important feature to achieve anti-fouling performance (*vide infra*). The content of DMAPS

277 at the near-surface of membranes increased with increasing grafting time, indicating higher  
278 grafting density and thicker brushes. Fig. 3E reports the ATR-FTIR spectra of all membranes.  
279 After polymerization, new bonds at  $3363\text{ cm}^{-1}$ ,  $1727\text{ cm}^{-1}$ , and  $1039\text{ cm}^{-1}$  appeared, which are  
280 associated to quaternary ammonium, C=O, and  $-\text{SO}_3$  groups, thus indicating the successful  
281 grafting of DMAPS on the surfaces of M2-M4.

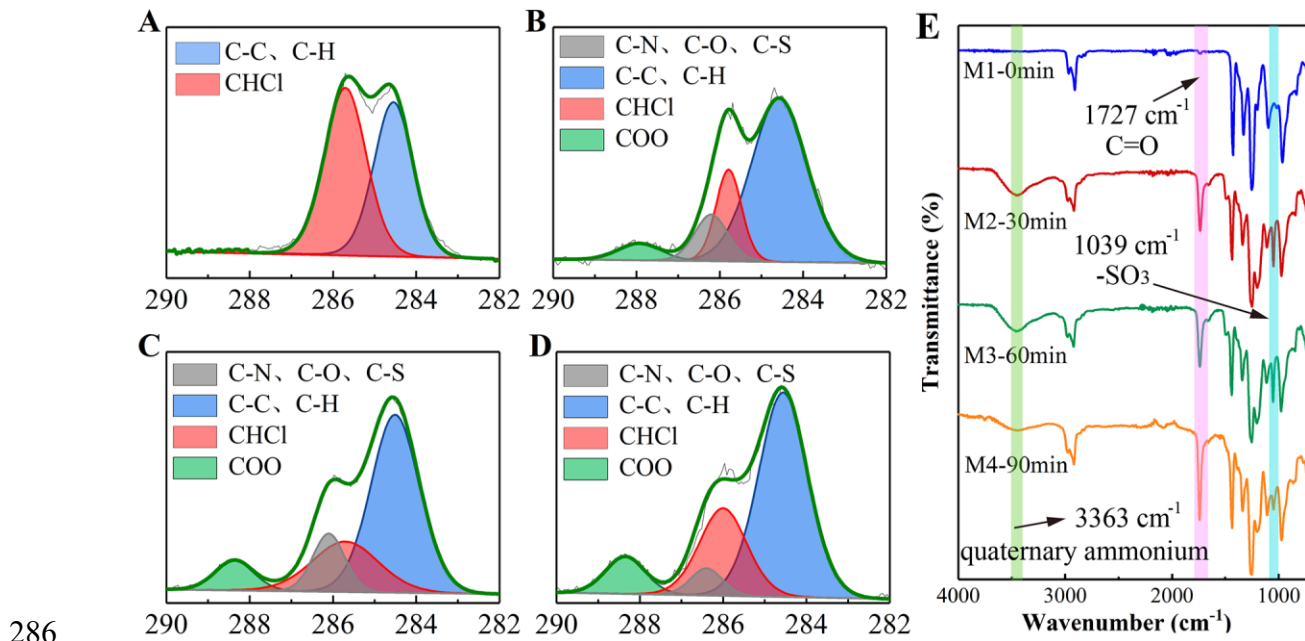
282 **Table 1.** Element atom percentages and mole fraction of DMAPS at the near-surface for all  
283 membranes.

Membrane ID	C (%)	Cl (%)	O (%)	N (%)	S (%)	$X^{\text{DMAPS}}$ (%)
M1-0min	66.49	33.01	0.50	-	-	-
M2-30min	81.78	11.86	5.87	0.25	0.24	23.69
M3-60min	70.54	11.10	16.07	1.16	1.13	25.77
M4-90min	84.52	6.74	8.28	0.20	0.26	26.39

284

285



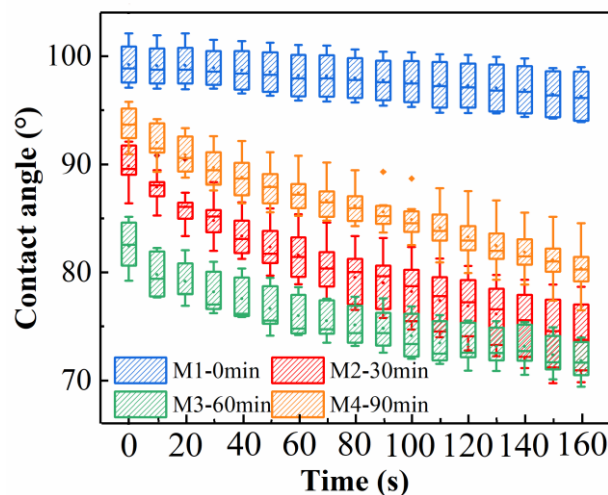


286  
287 **Fig. 3.** C 1s peak curve-fitting of XPS spectra for M1-M4: (A) M1-0 min, (B) M2-30min, (C)  
288 M3-60 min, (D) M4-90 min. And (E) ATR-FTIR spectra of M1-M4.

289

### 290 3.3. Membrane surface wettability

291 The behavior of water contact angles on the surface of M1-M4 as a function of time is  
292 presented in Fig. 4. Grafting zwitterionic DMAPS to membrane surface decreased the water  
293 contact angles and improved the wettability. After a short grafting time of 30 min, the initial  
294 contact angle was reduced from  $99.2 \pm 2.2^\circ$  (M1-0 min) to  $89.9 \pm 1.9^\circ$  (M2-30 min), and then to  
295  $82.4 \pm 2.5^\circ$  for M3-60 min. This result is attributed to the strong electrostatic interaction of  
296 DMAPS brushes with water molecules [73]. Extending the grafting time to 90 min, the  
297 wettability did not further improve, even though higher grafting density and thicker brushes were  
298 obtained. We attribute this phenomenon to the influence of the surface roughness. The  $R_q$   
299 roughness value of M4-90 min was remarkably larger than that of M3, which may reduce the  
300 wetting ability of the membrane surface [74]. Other studies observed similar phenomena [75].



301  
 302 **Fig. 4.** The behavior of water contact angles on the surface of the membranes as a function of  
 303 time. For each membrane sample, 4-12 different locations on the surface were detected.

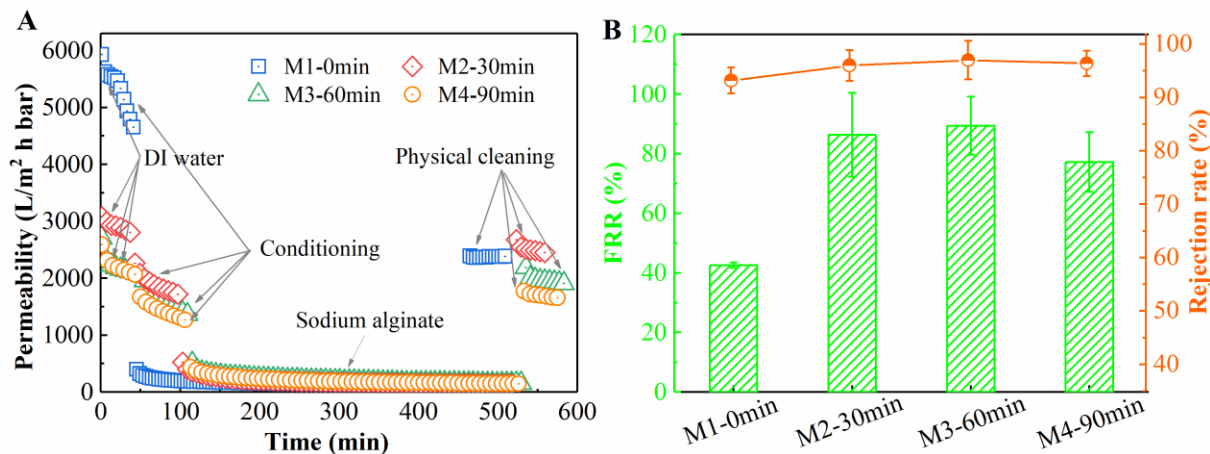
304

### 305 **3.4. Transport performance**

306 The permeabilities of M1-M4 are illustrated in Fig. 5A. As also reported by others in the  
 307 literature, surface grafting reduced the pure water permeability (PWP), likely because the  
 308 DMAPS brushes obstructed the pores on membrane surface, consistent with the above discussion  
 309 [22, 71]. The longer the grafting time, the larger the reduction of PWP. Although wettability is  
 310 an important factor affecting the membrane PWP, the effect of surface morphology was more  
 311 important in this experiment. However, one should note that even if the PWP was lower for  
 312 grafted membranes compared to the pristine membrane M1, its values were still high for all the  
 313 membranes:  $2872.3 \text{ L m}^{-2} \text{ h}^{-1} \text{ bar}^{-1}$  for M2,  $2134.1 \text{ L m}^{-2} \text{ h}^{-1} \text{ bar}^{-1}$  for M3, and  $2121.8 \text{ L m}^{-2} \text{ h}^{-1}$   
 314  $\text{bar}^{-1}$  for M4, thanks to the high performance of the PVC-PolarClean system, the reason of which  
 315 has been explored and analyzed comprehensively in our previous work [55].

316 The membrane flux recovery ratios (FRR) and SA rejection rates are shown in Fig. 5B. The  
317 SA rejection rates were all larger than 93 % because of the small average pore size diameter and  
318 narrow pore size distribution (see in Table 1). The average pore diameter of pristine membrane  
319 M1-0 min was 18.7 nm, and the SA particle size lies mostly in the range 15-80 nm, on the basis  
320 of its molecular weight distribution [76]. Longer grafting time ensured smaller surface pore  
321 diameter and surface porosity, thus improved the rejection rate from  $93.2 \pm 2.4$  % (M1), to  $96.0$   
322  $\pm 2.3$  % (M2),  $97.0 \pm 3.6$  % (M3), and  $96.4 \pm 2.4$  % (M4).

323 The anti-fouling property is of vital importance for UF membrane application and the main  
324 objective of this study. After the 7-h fouling stage, DI water physical washing for 3 min was  
325 employed to assess the membrane anti-fouling behavior. The FRR for pristine M1 was  $42.6 \pm$   
326  $0.9$  %. After surface grafting of zwitterionic DMAPS polymers, the FRR increased significantly.  
327 On the one hand, this phenomenon may be attributed to the hydration layer formed around the  
328 zwitterionic DMAPS brushes. On the other hand, the foulants were also repelled by polymer  
329 brushes because of steric hindrance [17]. It is interesting to note that M2-30 min, even if  
330 associated with the shortest investigated grafting time, exhibited an important improvement of  
331 FRR (86.4 %), indicating uniform coverage of DMAPS layer on membrane surface, and  
332 demonstrating the high efficiency of DMAPS to improve antifouling properties. M3-60 min  
333 showed a slightly increased FRR (89.4 %) with respect to M2, but when extending the grafting  
334 time to 90 min, the anti-fouling property declined with a FRR of 77.2 %. This phenomenon was  
335 consistent with the poor wettability of M4 attributed to the rougher surface.  $DR_t$ ,  $DR_r$ , and  $DR_{ir}$   
336 ratios are shown in Fig. S4 (SI).



337  
 338 **Fig. 5.** (A) Permeability with time for M1-0 min, M2-30 min, M3-60 min, and M4-90 min. (B)  
 339 SA rejection rates and flux recovery ratios (FRR) of M1-M4. The transport performance  
 340 experiment of every type of membrane was repeated at least twice.

341  
 342 **3.5. Membrane-foulant physicochemical interactions**

343 The surface tension parameters of all membranes and model SA particles were estimated from  
 344 contact angle measurements and are summarized in Table 2. The contact angles of three probe  
 345 liquids (water, diiodomethane, and formamide) are listed in Table S1. At least 5 measurements  
 346 for each sample were conducted to acquire the final average contact angle values shown in Table  
 347 S2. The calculation details are listed in Text S4 (SI). It was found that after surface grafting of  
 348 zwitterionic DMAPS polymers, the electron acceptor component ( $\gamma^+$ ) slightly increased, while  
 349 the electron donor component ( $\gamma^-$ ) increased importantly. This is because that the  $-\text{SO}_3$  group of  
 350 DMAPS is negatively charged in water, and can enhance the electron donating capability, hence  
 351 the hydrophilicity of the membrane surface [77].

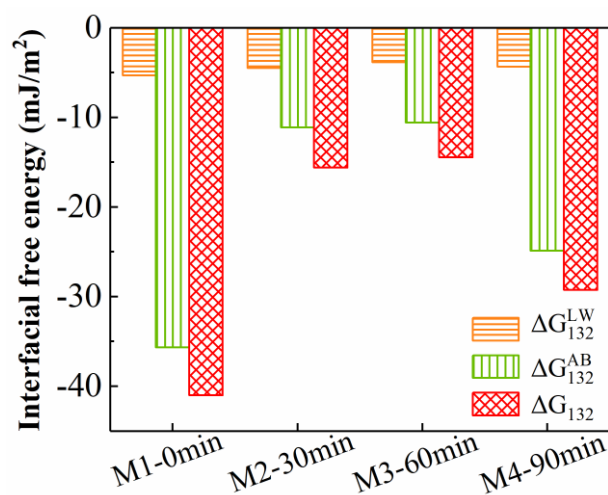
352 **Table 2.** The surface tension parameters of all membranes and SA particles.

Item	Surface tension parameters (mJ/m <sup>2</sup> )				
	$\gamma^{LW}$	$\gamma^-$	$\gamma^+$	$\gamma^{AB}$	$\gamma^{TOT}$
M1-0 min	42.028	0.037	0.000	0.011	42.039
M2-30 min	38.448	2.426	0.023	0.477	38.925
M3-60 min	35.821	2.679	0.093	0.997	36.818
M4-90 min	37.866	0.671	0.027	0.267	38.134
SA particles	37.647	9.706	0.669	5.097	42.744

353

354 The interfacial free energy between membrane surface and the SA particles was thus  
355 calculated via the surface tension parameters and equations (5-7), and the results are depicted in  
356 Fig. 6. The total interaction free energy ( $\Delta G_{132}$ ) is the combination of the Lifshitz–van der Waals  
357 (LW) and the Lewis acid–base (AB) interaction energies. A positive value indicates repulsive  
358 interaction, while negative value indicates attractive interactions. The more negative is the  
359 interaction, the more it is attractive, and the membrane surface is more likely to be fouled or  
360 unlikely to be efficiently cleaned after fouling [68, 78]. For M1-M4, their interaction energies  
361 with SA particles were all negative, indicating that the SA particles tend to attach on membrane  
362 surfaces in all systems. However, after surface grafting of DMAPS, M2-M4 showed a much  
363 low absolute values of  $\Delta G_{132}$ , implying the zwitterionic DMAPS polymer brushes effectively  
364 reduced the attractive interactions of foulants on the membrane surfaces, thus decreasing the  
365 likelihood of foulant attachment and improving membrane anti-fouling properties. Moreover, we  
366 found that the Lewis acid–base interaction energy ( $\Delta G_{132}^{AB}$ ) was much more negative than the  
367 Lifshitz–van der Waals interaction energy ( $\Delta G_{132}^{LW}$ ), and that the parameter  $\Delta G_{132}^{LW}$  underwent little  
368 change after surface grafting, while  $\Delta G_{132}^{AB}$  dramatically increased. Therefore, the Lewis

369 acid–base interaction energy ( $\Delta G_{132}^{AB}$ ) played a key role in the membrane fouling process. In  
370 summary, the main mechanism by which DMAPS polymer brushes enhanced the anti-fouling  
371 property of the membrane is by increasing the Lewis acid-base interaction energy. The  
372 relationship between  $\Delta G_{132}$  and water contact angle, as well as between  $\Delta G_{132}$  and FRR values, is  
373 presented in Fig. S5 (SI), showing a significant correlation, which indicates the suitable  
374 applicability of the XDLVO theory to predict and explain the membrane fouling behavior.



375  
376 **Fig. 6.** Total interaction energies ( $\Delta G_{132}$ ), Lifshitz–van der Waals interaction energies ( $\Delta G_{132}^{LW}$ )  
377 and Lewis acid–base (AB) interaction energies ( $\Delta G_{132}^{AB}$ ) between the membranes and SA particles  
378 in aqueous solution.

#### 379 4. Conclusion

380 On the basis of our previous study [55], green solvent PolarClean was utilized to fabricate  
381 PVC membranes with high permeabilities and foulants rejection rates. This work is aimed at  
382 improving their anti-fouling properties via environmentally friendly method. Zwitterionic  
383 DMAPS polymers were grafted on the membrane surface by ARGET-ATRP method with lower

384 environment impacts compared to traditional grafting methods. The XDLVO theory revealed  
385 that these polymer brushes could significantly reduce the interactions between membrane and  
386 foulants, especially those related to hydrophobic effects, thus promoting the membrane anti-  
387 fouling property. Other reports typically proposed grafting-based modification by pre-coating the  
388 surface with biophenols (*e.g.*, polydopamine, tannic acid) [17, 24, 25, 79-81]. However, this  
389 approach dramatically decrease the permeability of UF membranes, while increasing the  
390 complexity and cost of membrane fabrication. Instead, our study demonstrate the direct  
391 utilization of the chlorine atoms of the membrane backbones as effective initiation sites for the  
392 polymerization, greatly improving the anti-fouling performance while retaining membrane high  
393 permeability to the maximum extent.

394 The optimized grafting time was 30 min, and the related membrane exhibited very high  
395 performance: pure water permeability of  $2872.3 \text{ L m}^{-2} \text{ h}^{-1} \text{ bar}^{-1}$ , flux recovery rate of 86.4 %  
396 after a 7-hour SA fouling phase and foulant particle rejection of 96.0 %. This work achieved both  
397 green production and improved membrane performance, representing a successful exploration of  
398 sustainable chemistry and engineering toward membrane manufacturing. Further study should be  
399 directed to utilize this membrane in wastewater treatment, evaluating its anti-fouling and anti-  
400 bacterial properties in practical application.

401

#### 402 **CRedit authorship contribution statement**

403 **Wancen Xie:** Investigation, Validation, Formal analysis, Visualization, Data curation, Writing  
404 - original draft. **Alberto Tiraferri:** Formal analysis, Writing - review & editing. **Xuanyu Ji:**  
405 Validation, Formal analysis, Investigation. **Chen Chen:** Writing. **Yuhua Bai:** Writing. **John C.**

406 **Crittenden:** Writing. **Baicang Liu:** Conceptualization, Supervision, Formal analysis, Writing  
407 review & editing.

#### 408 **Declaration of competing interest**

409 The authors declare that they have no known competing financial interests or personal  
410 relationships that could have appeared to influence the work reported in this paper.

#### 411 **Acknowledgments**

412 This work was supported by the National Natural Science Foundation of China (52070134,  
413 51678377), and Sichuan University and Yibin City People's Government strategic cooperation  
414 project (2019CDYB-25). We would like to thank the Institute of New Energy and Low-Carbon  
415 Technology, Sichuan University, for SEM-EDS measurement. The authors acknowledge Solvay  
416 Specialty Polymers for providing PolarClean.

#### 417 **Appendix A. Supplementary material**

418 The following is the supplementary material related to this article:

419 Surface tension parameters of probe liquids (Table S1); Contact angles of all membranes and  
420 SA foulants (Table S2); Values of pore diameters information for all membranes (Table S3);  
421 Ternary phase diagram of PVC with PolarClean, DMAc and NMP used as solvent and DI water  
422 as nonsolvent (Fig. S1). SEM images of PVC membrane surface morphologies obtained with  
423 different grafting times: 120 min and 180 min (Fig. S2). XPS spectra of PVC membranes  
424 obtained with different grafting time (Fig. S3);  $DR_r$ ,  $DR_{ir}$ , and  $DR_t$  for all membranes obtained  
425 with different grafting time (Fig. S4); (A) Correlation between the total interaction energy  
426 ( $\Delta G_{132}$ ) and FRR. (B) Correlation between the total interaction energy ( $\Delta G_{132}$ ) and water contact  
427 angles (Fig. S5).



428 **References**

429 [1] Y. Saeki, T. Emura, Technical progresses for PVC production, *Prog. Polym. Sci.* 27 (2002)  
430 2055-2131.

431 [2] S. Moulay, Chemical modification of poly(vinyl chloride)—Still on the run, *Prog. Polym.*  
432 *Sci.* 35 (2010) 303-331.

433 [3] J. A. Xu, Z. L. Xu, Poly(vinyl chloride) (PVC) hollow fiber ultrafiltration membranes  
434 prepared from PVC/additives/solvent, *J. Membr. Sci.* 208 (2002) 203-212.

435 [4] Y. Zhang, X. Tong, B. Zhang, C. Zhang, H. Zhang, Y. Chen, Enhanced permeation and  
436 antifouling performance of polyvinyl chloride (PVC) blend Pluronic F127 ultrafiltration  
437 membrane by using salt coagulation bath (SCB), *J. Membr. Sci.* 548 (2018) 32-41.

438 [5] T. Ahmad, C. Guria, A. Mandal, Optimal synthesis and operation of low-cost polyvinyl  
439 chloride/bentonite ultrafiltration membranes for the purification of oilfield produced water, *J.*  
440 *Membr. Sci.* 564 (2018) 859-877.

441 [6] X. Fan, Y. Su, X. Zhao, Y. Li, R. Zhang, J. Zhao, Z. Jiang, J. Zhu, Y. Ma, Y. Liu,  
442 Fabrication of polyvinyl chloride ultrafiltration membranes with stable antifouling property by  
443 exploring the pore formation and surface modification capabilities of polyvinyl formal, *J.*  
444 *Membr. Sci.* 464 (2014) 100-109.

445 [7] D. Rana, T. Matsuura, Surface Modifications for Antifouling Membranes, *Chem. Rev.* 110  
446 (2010) 2448-2471.

- 447 [8] B. Liu, C. Chen, W. Zhang, J. Crittenden, Y. Chen, Low-cost antifouling PVC  
448 ultrafiltration membrane fabrication with Pluronic F 127: Effect of additives on properties and  
449 performance, *Desalination* 307 (2012) 26-33.
- 450 [9] Q. Wu, W. Xie, H. Wu, L. Wang, S. Liang, H. Chang, B. Liu, Effect of volatile solvent and  
451 evaporation time on formation and performance of PVC/PVC-g-PEGMA blended membranes,  
452 *RSC Advances* 9 (2019) 34486-34495.
- 453 [10] S.-Y. Wang, L.-F. Fang, L. Cheng, S. Jeon, N. Kato, H. Matsuyama, Novel ultrafiltration  
454 membranes with excellent antifouling properties and chlorine resistance using a poly(vinyl  
455 chloride)-based copolymer, *J. Membr. Sci.* 549 (2018) 101-110.
- 456 [11] L. Zheng, J. Wang, D. Yu, Y. Zhang, Y. Wei, Preparation of PVDF-CTFE hydrophobic  
457 membrane by non-solvent induced phase inversion: Relation between polymorphism and phase  
458 inversion, *J. Membr. Sci.* 550 (2018) 480-491.
- 459 [12] N. Singh, Z. Chen, N. Tomer, S. R. Wickramasinghe, N. Soice, S. M. Husson,  
460 Modification of regenerated cellulose ultrafiltration membranes by surface-initiated atom  
461 transfer radical polymerization, *J. Membr. Sci.* 311 (2008) 225-234.
- 462 [13] C. J. Porter, J. R. Werber, C. L. Ritt, Y.-F. Guan, M. Zhong, M. Elimelech, Controlled  
463 grafting of polymer brush layers from porous cellulosic membranes, *J. Membr. Sci.* 596 (2020)  
464 117719.
- 465 [14] J. F. Hester, P. Banerjee, Y. Y. Won, A. Akthakul, M. H. Acar, A. M. Mayes, ATRP of  
466 Amphiphilic Graft Copolymers Based on PVDF and Their Use as Membrane Additives,  
467 *Macromolecules* 35 (2002) 7652-7661.

468 [15] F. Galiano, A. Figoli, S. A. Deowan, D. Johnson, S. A. Altinkaya, L. Veltri, G. De Luca,  
469 R. Mancuso, N. Hilal, B. Gabriele, J. Hoinkis, A step forward to a more efficient wastewater  
470 treatment by membrane surface modification via polymerizable bicontinuous microemulsion, J.  
471 Membr. Sci. 482 (2015) 103-114.

472 [16] Y.-Y. Cheng, C.-H. Du, C.-J. Wu, K.-X. Sun, N.-P. Chi, Improving the hydrophilic and  
473 antifouling properties of poly(vinyl chloride) membranes by atom transfer radical polymerization  
474 grafting of poly(ionic liquid) brushes, Polym. Adv. Technol. 29 (2018) 623-631.

475 [17] D. M. Davenport, J. Lee, M. Elimelech, Efficacy of antifouling modification of  
476 ultrafiltration membranes by grafting zwitterionic polymer brushes, Sep. Purif. Technol. 189  
477 (2017) 389-398.

478 [18] W. Chen, Y. Su, J. Peng, X. Zhao, Z. Jiang, Y. Dong, Y. Zhang, Y. Liang, J. Liu, Efficient  
479 Wastewater Treatment by Membranes through Constructing Tunable Antifouling Membrane  
480 Surfaces, Environ. Sci. Technol. 45 (2011) 6545-6552.

481 [19] J. Jiang, P. Zhang, L. Zhu, B. Zhu, Y. Xu, Improving antifouling ability and  
482 hemocompatibility of poly(vinylidene fluoride) membranes by polydopamine-mediated ATRP, J.  
483 Mater. Chem. B 3 (2015) 7698-7706.

484 [20] J.-H. Li, M.-Z. Li, J. Miao, J.-B. Wang, X.-S. Shao, Q.-Q. Zhang, Improved surface  
485 property of PVDF membrane with amphiphilic zwitterionic copolymer as membrane additive,  
486 Appl. Surf. Sci. 258 (2012) 6398-6405.

487 [21] Y.-F. Zhao, P.-B. Zhang, J. Sun, C.-J. Liu, Z. Yi, L.-P. Zhu, Y.-Y. Xu, Versatile  
488 antifouling polyethersulfone filtration membranes modified via surface grafting of zwitterionic

489 polymers from a reactive amphiphilic copolymer additive, *J. Colloid Interface Sci.* 448 (2015)  
490 380-388.

491 [22] W.-W. Yue, H.-J. Li, T. Xiang, H. Qin, S.-D. Sun, C.-S. Zhao, Grafting of zwitterion from  
492 polysulfone membrane via surface-initiated ATRP with enhanced antifouling property and  
493 biocompatibility, *J. Membr. Sci.* 446 (2013) 79-91.

494 [23] P.-S. Liu, Q. Chen, X. Liu, B. Yuan, S.-S. Wu, J. Shen, S.-C. Lin, Grafting of Zwitterion  
495 from Cellulose Membranes via ATRP for Improving Blood Compatibility, *Biomacromolecules*  
496 10 (2009) 2809-2816.

497 [24] C. Cheng, S. Li, W. Zhao, Q. Wei, S. Nie, S. Sun, C. Zhao, The hydrodynamic  
498 permeability and surface property of polyethersulfone ultrafiltration membranes with mussel-  
499 inspired polydopamine coatings, *J. Membr. Sci.* 417-418 (2012) 228-236.

500 [25] H. C. Yang, K. J. Liao, H. Huang, Q. Y. Wu, L. S. Wan, Z. K. Xu, Mussel-inspired  
501 modification of a polymer membrane for ultra-high water permeability and oil-in-water emulsion  
502 separation, *J. Mater. Chem. A* 2 (2014) 10225-10230.

503 [26] D. S. Kim, J. S. Kang, Y. M. Lee, Microfiltration of activated sludge using modified PVC  
504 membranes: Effect of pulsing on flux recovery, *Sep. Sci. Technol.* 38 (2003) 591-612.

505 [27] J. Seok Kang, S. Hoon Lee, H. Huh, J. Kie Shim, Y. Moo Lee, Preparation of chlorinated  
506 poly(vinyl chloride)-g-poly(N-vinyl-2-pyrrolidinone) membranes and their water permeation  
507 properties, *J. Appl. Polym. Sci.* 88 (2003) 3188-3195.

- 508 [28] A. Siekierka, J. Wolska, W. Kujawski, M. Bryjak, Modification of poly(vinyl chloride)  
509 films by aliphatic amines to prepare anion-exchange membranes for Cr (VI) removal, *Sep. Sci.*  
510 *Technol.* 53 (2018) 1191-1197.
- 511 [29] L. Zhang, M. Tang, J. Zhang, P. Zhang, J. Zhang, L. Deng, C. Lin, A. Dong, One simple  
512 and stable coating of mixed-charge copolymers on poly(vinyl chloride) films to improve  
513 antifouling efficiency, *J. Appl. Polym. Sci.* 134 (2017).
- 514 [30] J. Dai, Y. Dong, C. Yu, Y. Liu, X. Teng, A novel Nafion-g-PSBMA membrane prepared  
515 by grafting zwitterionic SBMA onto Nafion via SI-ATRP for vanadium redox flow battery  
516 application, *J. Membr. Sci.* 554 (2018) 324-330.
- 517 [31] J. Zhang, J. Yuan, Y. Yuan, X. Zang, J. Shen, S. Lin, Platelet adhesive resistance of  
518 segmented polyurethane film surface-grafted with vinyl benzyl sulfo monomer of ammonium  
519 zwitterions, *Biomaterials* 24 (2003) 4223-4231.
- 520 [32] M. Zhou, H. Liu, J. E. Kilduff, R. Langer, D. G. Anderson, G. Belfort, High-Throughput  
521 Membrane Surface Modification to Control NOM Fouling, *Environ. Sci. Technol.* 43 (2009)  
522 3865-3871.
- 523 [33] J. B. Zimmerman, P. T. Anastas, H. C. Erythropel, W. Leitner, Designing for a green  
524 chemistry future, *Science* 367 (2020) 397-400.
- 525 [34] L. Liu, H. Chen, F. Yang, Enhancing membrane performance by blending ATRP grafted  
526 PMMA-TiO<sub>2</sub> or PMMA-PSBMA-TiO<sub>2</sub> in PVDF, *Sep. Purif. Technol.* 133 (2014) 22-31.

527 [35] L. Zhang, Y. Lin, L. Cheng, Z. Yang, H. Matsuyama, A comprehensively fouling- and  
528 solvent-resistant aliphatic polyketone membrane for high-flux filtration of difficult oil-in-water  
529 micro- and nanoemulsions, *J. Membr. Sci.* 582 (2019) 48-58.

530 [36] Y.-H. Zhao, K.-H. Wee, R. Bai, A Novel Electrolyte-Responsive Membrane with Tunable  
531 Permeation Selectivity for Protein Purification, *ACS Appl. Mater. Inter.* 2 (2010) 203-211.

532 [37] L.-J. Zhu, F. Liu, X.-M. Yu, A.-L. Gao, L.-X. Xue, Surface zwitterionization of  
533 hemocompatible poly(lactic acid) membranes for hemodiafiltration, *J. Membr. Sci.* 475 (2015)  
534 469-479.

535 [38] Y. Zhang, Z. Wang, W. Lin, H. Sun, L. Wu, S. Chen, A facile method for polyamide  
536 membrane modification by poly(sulfobetaine methacrylate) to improve fouling resistance, *J.*  
537 *Membr. Sci.* 446 (2013) 164-170.

538 [39] C. Liu, A. F. Faria, J. Ma, M. Elimelech, Mitigation of Biofilm Development on Thin-  
539 Film Composite Membranes Functionalized with Zwitterionic Polymers and Silver  
540 Nanoparticles, *Environ. Sci. Technol.* 51 (2017) 182-191.

541 [40] K. Matyjaszewski, Atom Transfer Radical Polymerization (ATRP): Current Status and  
542 Future Perspectives, *Macromolecules* 45 (2012) 4015-4039.

543 [41] H. Wu, T. Li, B. Liu, C. Chen, S. Wang, J. C. Crittenden, Blended PVC/PVC-g-PEGMA  
544 ultrafiltration membranes with enhanced performance and antifouling properties, *Appl. Surf. Sci.*  
545 455 (2018) 987-996.

546 [42] W. Xie, T. Li, C. Chen, H. Wu, S. Liang, H. Chang, B. Liu, E. Drioli, Q. Wang, J. C.  
547 Crittenden, Using the Green Solvent Dimethyl Sulfoxide To Replace Traditional Solvents Partly

548 and Fabricating PVC/PVC-g-PEGMA Blended Ultrafiltration Membranes with High  
549 Permeability and Rejection, *Ind. Eng. Chem. Res.* 58 (2019) 6413-6423.

550 [43] P. Kryszewski, K. Matyjaszewski, Kinetics of Atom Transfer Radical Polymerization, *Eur.*  
551 *Polym. J.* 89 (2017) 482-523.

552 [44] K. Matyjaszewski, Advanced Materials by Atom Transfer Radical Polymerization, *Adv.*  
553 *Mater.* 30 (2018) 1706441.

554 [45] T. G. Ribelli, M. Fantin, J.-C. Daran, K. F. Augustine, R. Poli, K. Matyjaszewski,  
555 Synthesis and Characterization of the Most Active Copper ATRP Catalyst Based on Tris (4-  
556 dimethylaminopyridyl)methyl amine, *J. Am. Chem. Soc.* 140 (2018) 1525-1534.

557 [46] Z. Zhang, X. Wang, K. C. Tam, G. Sèbe, A comparative study on grafting polymers from  
558 cellulose nanocrystals via surface-initiated atom transfer radical polymerization (ATRP) and  
559 activator re-generated by electron transfer ATRP, *Carbohydr. Polym.* 205 (2019) 322-329.

560 [47] S. T. Chow, T. L. Ng, The biodegradation of N-methyl-2-pyrrolidone in water by sewage  
561 bacteria, *Water Res.* 17 (1983) 117-118.

562 [48] D. J. C. Constable, P. J. Dunn, J. D. Hayler, G. R. Humphrey, J. L. Leazer, Jr., R. J.  
563 Linderman, K. Lorenz, J. Manley, B. A. Pearlman, A. Wells, A. Zaks, T. Y. Zhang, Key green  
564 chemistry research areas - a perspective from pharmaceutical manufacturers, *Green Chem.* 9  
565 (2007) 411-420.

566 [49] C. Wang, C. Huang, Y. Wei, Q. Zhu, W. Tian, Q. Zhang, Short-term exposure to  
567 dimethylformamide and the impact on digestive system disease: An outdoor study for volatile  
568 organic compound, *Environ. Pollut.* 190 (2014) 133-138.

569 [50] P. Anastas, N. Eghbali, Green chemistry: principles and practice, Chem. Soc. Rev. 39  
570 (2010) 301-312.

571 [51] C. Capello, U. Fischer, K. Hungerbuehler, What is a green solvent? A comprehensive  
572 framework for the environmental assessment of solvents, Green Chem. 9 (2007) 927-934.

573 [52] F. P. Byrne, S. Jin, G. Paggiola, T. H. M. Petchey, J. H. Clark, T. J. Farmer, A. J. Hunt, C.  
574 Robert McElroy, J. Sherwood, Tools and techniques for solvent selection: green solvent  
575 selection guides, Sustainable Chem. Processes 4 (2016) 1-24.

576 [53] D. Ji, C. Xiao, S. An, K. Chen, Y. Gao, F. Zhou, T. Zhang, Completely green and  
577 sustainable preparation of PVDF hollow fiber membranes via melt-spinning and stretching  
578 method, J. Hazard. Mater. 398 (2020) 122823.

579 [54] C. J. Clarke, W.-C. Tu, O. Levers, A. Brohl, J. P. Hallett, Green and Sustainable Solvents  
580 in Chemical Processes, Chem. Rev. 118 (2018) 747-800.

581 [55] W. Xie, A. Tiraferri, B. Liu, P. Tang, F. Wang, S. Chen, A. Figoli, L.-Y. Chu, First  
582 Exploration on a Poly(vinyl chloride) Ultrafiltration Membrane Prepared by Using the  
583 Sustainable Green Solvent PolarClean, ACS Sustainable Chem. Eng. 8 (2020) 91-101.

584 [56] B. M. Pastore, M. J. Savelski, C. S. Slater, F. A. Richetti, Life cycle assessment of N-  
585 methyl-2-pyrrolidone reduction strategies in the manufacture of resin precursors, Clean Technol.  
586 Environ. Policy 18 (2016) 2635-2647.

587 [57] V. Faggian, P. Scanferla, S. Paulussen, S. Zuin, Combining the European chemicals  
588 regulation and an (eco)toxicological screening for a safer membrane development, J. Clean.  
589 Prod. 83 (2014) 404-412.



590 [58] H.-Y. Shiu, M. Lee, Y. Chao, K.-C. Chang, C.-H. Hou, P.-T. Chiueh, Hotspot analysis  
591 and improvement schemes for capacitive deionization (CDI) using life cycle assessment,  
592 *Desalination* 468 (2019) 114087.

593 [59] B. Simon, K. Bachtin, A. Kiliç, B. Amor, M. Weil, Proposal of a framework for scale-up  
594 life cycle inventory: A case of nanofibers for lithium iron phosphate cathode applications, *Integr.*  
595 *Environ. Asses.* 12 (2016) 465-477.

596 [60] L. Luciani, E. Goff, D. Lanari, S. Santoro, L. Vaccaro, Waste-minimised copper-catalysed  
597 azide–alkyne cycloaddition in PolarClean as a reusable and safe reaction medium, *Green Chem.*  
598 20 (2018) 183-187.

599 [61] L. Cseri, G. Szekely, Towards cleaner PolarClean: Efficient synthesis and extended  
600 applications of the polar aprotic solvent methyl 5-(dimethylamino)-2-methyl-5-oxopentanoate,  
601 *Green Chem.* 21 (2019) 4178-4188.

602 [62] N. T. Hassankiadeh, Z. Cui, J. H. Kim, D. W. Shin, S. Y. Lee, A. Sanguineti, V. Arcella,  
603 Y. M. Lee, E. Drioli, Microporous poly(vinylidene fluoride) hollow fiber membranes fabricated  
604 with PolarClean as water-soluble green diluent and additives, *J. Membr. Sci.* 479 (2015) 204-  
605 212.

606 [63] X. Dong, T. J. Jeong, E. Kline, L. Banks, E. Grulke, T. Harris, I. C. Escobar, Eco-friendly  
607 solvents and their mixture for the fabrication of polysulfone ultrafiltration membranes: An  
608 investigation of doctor blade and slot die casting methods, *J. Membr. Sci.* 614 (2020) 118510.

609 [64] C. Y. Tang, Y.-N. Kwon, J. O. Leckie, Effect of membrane chemistry and coating layer  
610 on physiochemical properties of thin film composite polyamide RO and NF membranes: I. FTIR

611 and XPS characterization of polyamide and coating layer chemistry, *Desalination* 242 (2009)  
612 149-167.

613 [65] Q. Wu, A. Tiraferri, H. Wu, W. Xie, B. Liu, Improving the Performance of PVDF/PVDF-  
614 g-PEGMA Ultrafiltration Membranes by Partial Solvent Substitution with Green Solvent  
615 Dimethyl Sulfoxide during Fabrication, *ACS Omega* 4 (2019) 19799-19807.

616 [66] B. Liu, C. Chen, T. Li, J. Crittenden, Y. Chen, High performance ultrafiltration membrane  
617 composed of PVDF blended with its derivative copolymer PVDF-g-PEGMA, *J. Membr. Sci.* 445  
618 (2013) 66-75.

619 [67] X. Zhao, Y. Su, W. Chen, J. Peng, Z. Jiang, Grafting perfluoroalkyl groups onto  
620 polyacrylonitrile membrane surface for improved fouling release property, *J. Membr. Sci.* 415  
621 (2012) 824-834.

622 [68] C. Liu, D. Song, W. Zhang, Q. He, X. Huangfu, S. Sun, Z. Sun, W. Cheng, J. Ma,  
623 Constructing zwitterionic polymer brush layer to enhance gravity-driven membrane performance  
624 by governing biofilm formation, *Water Res.* 168 (2020) 115181.

625 [69] T. Lin, B. Shen, W. Chen, X. Zhang, Interaction mechanisms associated with organic  
626 colloid fouling of ultrafiltration membrane in a drinking water treatment system, *Desalination*  
627 332 (2014) 100-108.

628 [70] C. J. van Oss, Acid—base interfacial interactions in aqueous media, *Colloids and Surfaces*  
629 A: Physicochemical and Engineering Aspects 78 (1993) 1-49.

630 [71] N. Shahkaramipour, A. Jafari, T. Tran, C. M. Stafford, C. Cheng, H. Lin, Maximizing the  
631 grafting of zwitterions onto the surface of ultrafiltration membranes to improve antifouling  
632 properties, *J. Membr. Sci.* 601 (2020) 117909.

633 [72] M. A. U. R. Alvi, M. W. Khalid, N. M. Ahmad, M. B. K. Niazi, M. N. Anwar, M. Batool,  
634 W. Cheema, S. Rafiq, Polymer concentration and solvent variation correlation with the  
635 morphology and water filtration analysis of polyether sulfone microfiltration membrane, *Adv.*  
636 *Polym. Tech.* 2019 (2019) 1-11.

637 [73] J. B. Schlenoff, Zwitteration: Coating Surfaces with Zwitterionic Functionality to Reduce  
638 Nonspecific Adsorption, *Langmuir* 30 (2014) 9625-9636.

639 [74] C. Meringolo, T. F. Mastropietro, T. Poerio, E. Fontananova, G. De Filpo, E. Curcio, G.  
640 Di Profio, Tailoring PVDF Membranes Surface Topography and Hydrophobicity by a  
641 Sustainable Two-Steps Phase Separation Process, *ACS Sustainable Chem. Eng.* 6 (2018) 10069-  
642 10077.

643 [75] Q. Liu, A. A. Patel, L. Liu, Superhydrophilic and Underwater Superoleophobic  
644 Poly(sulfobetaine methacrylate)-Grafted Glass Fiber Filters for Oil–Water Separation, *ACS*  
645 *Appl. Mater. Inter.* 6 (2014) 8996-9003.

646 [76] W. Shuai, L. Tong, C. Chen, L. Baicang, J. C. Crittenden, PVDF ultrafiltration  
647 membranes of controlled performance via blending PVDF-g-PEGMA copolymer synthesized  
648 under different reaction times, *Front. Environ. Sci. Eng.* 12 (2018) 3.

649 [77] H. Wang, M. Park, H. Liang, S. Wu, I. J. Lopez, W. Ji, G. Li, S. A. Snyder, Reducing  
650 ultrafiltration membrane fouling during potable water reuse using pre-ozonation, *Water Res.* 125  
651 (2017) 42-51.

652 [78] N. Subhi, A. R. D. Verliefde, V. Chen, P. Le-Clech, Assessment of physicochemical  
653 interactions in hollow fibre ultrafiltration membrane by contact angle analysis, *J. Membr. Sci.*  
654 403-404 (2012) 32-40.

655 [79] G. Li, B. Liu, L. Bai, Z. Shi, X. Tang, J. Wang, H. Liang, Y. Zhang, B. Van der Bruggen,  
656 Improving the performance of loose nanofiltration membranes by poly-dopamine/zwitterionic  
657 polymer coating with hydroxyl radical activation, *Sep. Purif. Technol.* 238 (2020) 116412.

658 [80] Y. Xu, D. Guo, T. Li, Y. Xiao, L. Shen, R. Li, Y. Jiao, H. Lin, Manipulating the mussel-  
659 inspired co-deposition of tannic acid and amine for fabrication of nanofiltration membranes with  
660 an enhanced separation performance, *J. Colloid Interface Sci.* 565 (2020) 23-34.

661 [81] X. Zhang, J. Tian, S. Gao, W. Shi, Z. Zhang, F. Cui, S. Zhang, S. Guo, X. Yang, H. Xie,  
662 D. Liu, Surface functionalization of TFC FO membranes with zwitterionic polymers:  
663 Improvement of antifouling and salt-responsive cleaning properties, *J. Membr. Sci.* 544 (2017)  
664 368-377.

665